

## Article

# Wear Study of a Magnetron-Sputtered TiC/a-C Nanocomposite Coating under Media-Lubricated Oscillating Sliding Conditions

Johannes Schneider <sup>1,\*</sup> , Sven Ulrich <sup>2</sup>, Jörg Patscheider <sup>3</sup> and Michael Stueber <sup>2,\*</sup>

<sup>1</sup> Institute for Applied Materials (IAM-ZM), Karlsruhe Institute of Technology (KIT), Kaiserstrasse 12, 76021 Karlsruhe, Germany

<sup>2</sup> Institute for Applied Materials (IAM-AWP), Karlsruhe Institute of Technology (KIT), Hermann-von-Helmholtz-Platz 1, 76344 Eggenstein-Leopoldshafen, Germany; sven.ulrich@kit.edu

<sup>3</sup> Evatec AG, Hauptstrasse 1a, 9477 Trübbach, Switzerland; joerg.patscheider@evatecnet.com

\* Correspondence: johannes.schneider@kit.edu (J.S.); michael.stueber@kit.edu (M.S.)

**Abstract:** Friction and wear performance of non-reactively magnetron-sputtered hydrogen-free TiC/a-C coatings were characterized under lubricated oscillating sliding conditions against 100Cr6 steel. The friction mediators, isooctane, ethanol and distilled water, were chosen to address the actual trend of environmentally friendly green technologies in mobility and the potential use of carbon-based nanocomposite thin film materials for tribocomponents in contact with gasoline and alternative biofuels. Sliding pairs of the TiC/a-C coatings showed significantly reduced friction and wear compared to the reference materials under both unlubricated and lubricated conditions (when using the aforementioned media isooctane, ethanol and distilled water). Quasi-stationary friction coefficient of the TiC/a-C sliding pairs after running-in was almost independent of test conditions and could be traced back to self-lubrication as a result of the formation of a transfer layer on the steel counter body. Wear of the coatings based on micro-abrasion and tribochemical reaction was significantly influenced by the environmental conditions. Lowest wear was measured after tests in non-polar isooctane whereas highest wear was measured after tests in water.

**Keywords:** carbon-based nanocomposite; thin films; magnetron sputtering; tribology; wear; friction; wear mechanism



**Citation:** Schneider, J.; Ulrich, S.; Patscheider, J.; Stueber, M. Wear Study of a Magnetron-Sputtered TiC/a-C Nanocomposite Coating under Media-Lubricated Oscillating Sliding Conditions. *Coatings* **2022**, *12*, 446. <https://doi.org/10.3390/coatings12040446>

Academic Editor: Rubén González

Received: 21 February 2022

Accepted: 22 March 2022

Published: 25 March 2022

**Publisher's Note:** MDPI stays neutral with regard to jurisdictional claims in published maps and institutional affiliations.



**Copyright:** © 2022 by the authors. Licensee MDPI, Basel, Switzerland. This article is an open access article distributed under the terms and conditions of the Creative Commons Attribution (CC BY) license (<https://creativecommons.org/licenses/by/4.0/>).

## 1. Introduction

Carbon-based nanostructured composite thin films of the general form MeC/a-C (Me: transition metal, MeC: transition metal carbide phase, nanocrystalline; a-C: amorphous carbon phase) and their hydrogen-containing variants, MeC:H/a-C:H, have been intensively discussed as promising low-friction, wear-resistant materials in various tribological environments for low- to medium-temperature engineering applications for almost two decades [1–8]. Nanostructure design concepts and fundamental materials science aspects of such nanocomposite thin films have been continuously described in comprehensive reviews [9–15]. The synthesis and deposition of such thin films via physical vapor deposition has been addressed in detail in literature. Manifold reports are available for the non-reactive magnetron sputter co-deposition utilizing different combinations of multiple metal, graphite, compound and composite target arrangements [3,4,11–23]. Significant information has also been published for reactive magnetron sputter deposition processes, very often utilizing target configurations as mentioned above and reactive gases such as methane, acetylene and admixtures of hydrogen [2,11,22,24–30]. Various modified and hybrid physical vapor deposition (PVD)/Chemical Vapor Deposition– (CVD) processes based on sputtering processes have been discussed [1,5,6,15,31–35]). Pulsed magnetron

sputtering deposition technologies [36–40], especially novel high-power impulse magnetron sputtering (HIPIMS) [7,8,41–44], and cathodic arc evaporation, are currently gaining wider research interest [45–47].

The nanocomposite thin films considered in this article exhibit significant volume fractions of both the nanocrystalline carbide and amorphous carbon phases, while the distinction to the so-called metal-containing amorphous (hydrogenated) carbon coatings with low metal concentration and often lower crystallinity of the carbide phase is smooth and material-dependent [2,11,14,15]. The synthesis, growth, microstructure and phase formation and the impact of composition and microstructure on the thin film properties have been investigated both for hydrogen-free and hydrogen-containing thin film materials such as TiC/a-C [2–8,11,12,15–19,21,25,26,28–35,38–45], WC/a-C [19,21,22,27,32,34,44,48–51] and CrC<sub>x</sub>/a-C [19,28–30,52–54]. Other material combinations such as ZrC/a-C [55–58], NbC/a-C [59–61], VC/a-C [62–65], TaC/a-C [55,66–68] and more complex thin film designs, i.e., multiple elements containing coatings, integration of such layers into multilayer and gradient architectures, have been reported with less attention so far [14,69–73]. Among this class of promising engineering materials, metal carbide/amorphous carbon nanocomposite thin films in the system Ti-C(:H) have found widespread interest because the combination of a transition metal carbide and an amorphous carbon matrix phase allows for relatively easy thin film synthesis and microstructure and properties tailoring. Exemplarily, the formation of a two-phase nanocomposite structure in such systems is favored due to limited solubility of carbon in the lattice of a transition metal carbide, i.e., TiC, or when a maximum Ti vacancy concentration is exceeded in the TiC lattice. The constitution, chemical bonding, microstructural design and control, as well as the tuning of mechanical and tribological properties of TiC(:H)/a-C(:H) thin films have been systematically studied [9–15,74–76]. It is common understanding that both their friction and wear properties (like mechanical properties in general) are clearly dependent on the Ti:C concentration ratio, the volume fraction of both the nanocrystalline and amorphous phases, the grain size of the carbide phase and the thin films hardness, surface roughness and further characteristics, for example H/E and H<sup>3</sup>/E<sup>2</sup> ratios [1–5,9–15]. Basically, the correlation of friction and wear performances of TiC(:H)/a-C(:H) thin films with the Ti:C concentration ratio and the mentioned characteristics is widely independent of the thin film synthesis method, and this is similar for both hydrogen-free and hydrogenated thin films [1–5]. At higher Ti concentration (and larger volume fraction of the carbide phase), the hardness of the thin films is high, often reaching values close to those of pure TiC coatings (in the range of 30 GPa and higher), while the wear and friction performance is not always satisfactory (while naturally dependent on the tribological system under examination). In many studies, Ti-rich nanocomposite coatings exhibited higher values for wear and coefficients of friction. At higher carbon concentration (and larger volume fraction of the amorphous carbon phase), the hardness of the thin films is usually lower (in the range of 20 GPa and below), while the wear and friction values are significantly reduced. Depending on the testing conditions and related tribosystems, carbon-rich nanocomposite thin films typically show very low friction coefficients in the range of 0.15 and even below. A range for the carbon concentration, approximately between 60% and 75%, has been identified as a major specification to achieve wear-resistant low-friction nanocomposite coatings (see for example [1–5,9–15]). Such observations and conclusions are in principle also valid for other types of nanocrystalline metal carbide/amorphous carbon composite thin films when those are tested under similar conditions in wear studies.

The majority of published studies (especially those cited in this article so far) deal with pin-on-disc (ball-on-disc) experiments of such thin films under lubricated or unlubricated unidirectional sliding conditions. Frequently, the counterpart ball material is steel, mostly 100Cr6, while other materials such as cemented carbide (WC-Co), tungsten carbide, alumina, silicon nitride or others have also been used. The variation of reported experimental conditions is huge, and covers for example a wide range of normal loads (1–10 N, sometimes higher, up to 30 N), sliding distances (several 10 m up to 2000 m),

sliding speeds (0.005–0.3 m/s, in extreme cases even up to 0.5 m/s), diameters of the ball counter body (mostly 1–6 mm, sometimes up to 10 mm) or values for the radius of the wear tracks, resulting in different load scenarios, often with an initial Hertzian contact pressure in the GPa range (0.3 GPa up to 2 GPa, or higher). When experiments were carried out in humid air, the relative humidity is reported to be mostly in the range 20–80% (while in many articles this is not specified in detail). It has to be noted that often such conditions have been marked as dry conditions in literature, while those may be considered simply as unlubricated conditions. Most studies have been performed at ambient temperature and pressure, while few deal with wear studies and friction tests at higher temperature [4–11,16,21,24,30,38–44,49,52,55–57,61,66–70]. The wear mechanisms identified in tests carried out at ambient temperature and in humid air are abrasive wear and tribochemical reactions, resulting in third-body conditions; the constitution and microstructure of the nanocomposite thin films determine the predominant wear and friction scenario (dependent also on the tribosystem in general). At high carbon content (and thus larger volume fraction of the amorphous carbon phase), a carbon-based transfer layer can form on the counterpart body, leading to sustained self-lubrication events, accompanied by low friction coefficients and wear rates. Under specific conditions (i.e., high contact pressure and/or high sliding velocities), the temperature in the tribocontact zone can rise up to 350–400 °C and result in local graphitization of both the nanocomposite coating and the transfer layer, which can further contribute temporarily to self-lubrication.

The usage of various lubrication media such as water, oils, fuels and others in pin-on-disc tribological testing has been described for pure amorphous or diamond-like carbon coatings and for metal containing amorphous carbon coatings (usually for coatings with lower metal concentration (see exemplarily [77,78] and various articles in section B in [79], while fewer studies are available for nanocomposite carbide/amorphous carbon coatings with significant volume fraction of both phases. Zhang et al. [17] reported wear studies in pin-on-disc tests of TiC/a-C nanocomposite coatings against a steel ball counterpart (100Cr6) in both unlubricated (i.e., in air with 75% relative humidity, at 22 °C, specified as dry conditions) and lubricated conditions. In that investigation, the friction tests were carried out with a classical engine oil (Shell Helix 15–50). Under unlubricated test conditions, the friction coefficient showed a strong correlation with the Ti concentration of the coatings: it increased continuously with the Ti concentration. Such behavior is characteristic for many types of carbide/amorphous carbon thin films tested under similar conditions. It has been attributed to the impact of the Ti:C concentration ratio on the volume fractions of the crystalline carbide and the amorphous carbon phases, on the surface topography and the ability to form a lubricious, solid graphite layer in the tribocontact zone [17]. A TiC/a-C nanocomposite coating with 30 at.% Ti concentration showed different friction behavior when the test was conducted in oil lubrication. The friction coefficient was significantly reduced in comparison to the unlubricated condition; after a certain run-in period, it decreased moderately but continuously with the sliding distance. Zhang et al. explained that the oil lubrication prevented the formation of a graphite-rich layer in the contact zone, resulting in a different friction mechanism in comparison with the situation observed in humid air. A stable friction regime could be established, dependent on the coatings' surface topography (i.e., roughness), coating thickness and stability of the oil film between the sliding partners [17]. Keunecke et al. [30] presented a study on CrC/a-C:H thin films tested in oil-lubricated pin-on-disc experiments against 100Cr6 steel. A classical engine oil (SAE 0W-20) was used as lubricant in one experimental series, while the same oil containing specific additives to impact the tribochemistry and friction performance (i.e., MoDTC) was used in a second experimental series. The initial Hertzian contact pressure was set to a high load (2 GPa). All coatings (with systematically varied Cr:C concentration ratio) under examination showed low friction values in general, while the friction coefficients were even lower in test conditions applying the oil with additives. Keunecke et al. found, however, that the wear properties in contact with the additive-loaded oil were strongly dependent on the Cr:C concentration ratio, and they were optimum in their study in the

range of 50 at.% Cr content. They suggested that the interaction of the tribopartners with the additive should play a vital role for the friction and wear performance in such conditions. Mandal et al. [80] investigated the wear mechanisms of Cr-containing carbon coatings in a pin-on-disc test against 100Cr6 under lubrication with a synthetic engine oil (Mobil1 Extended Life™) containing polymer additives. They observed low friction coefficients, smooth friction curves with only short run-in phase and low wear of the coatings. They suggested a tribochemical reaction between the coating and the oil, resulting in the formation of a lubricious CrCl<sub>3</sub>-containing surface in the contact zone, as a major factor for achieving low friction and wear in the tested system.

Wear studies on oscillating (reciprocating) sliding friction, both unlubricated and lubricated, have been reported in detail for a variety of amorphous and diamond-like carbon coatings [79,81–89] and for metal-containing carbon coatings [90–95]. Less work has yet been published on the performance of MeC(H)/a-C:H thin films under reciprocating sliding friction conditions. Scharf and Singer demonstrated, for such conditions and three types of metal-carbide-containing amorphous carbon composite coatings, that the formation of an adherent transfer layer on the counterpart body and the transition from the run-in phase (accompanied with higher friction coefficient and wear) to a stationary friction state (at significantly reduced friction coefficient and wear rate) are both material and tribosystem dependent. Among the materials under examination, both TiC/a-C and TiC/a-C:H coatings exhibited low friction coefficients and wear rates in reciprocating sliding tests against sapphire and steel in dry and ambient air at room temperature (relative humidity: 2%–5%, or ~50%, respectively). Irrespective of humidity, the formation of a transfer layer occurred rapidly for these coatings, leading to a short run-in phase and a separation of counterpart material and original coating; sliding of the transfer film against the original coating surface occurred with a very low friction coefficient. The low friction, usually attributed to a specific coating, was (again) related to a third body interaction. Formation of such a transfer layer was much slower in the case of WC/a-C:H coatings, resulting in different run-in phase and initial friction and wear conditions [96]. Ciarsolo et al. investigated the friction and wear performance of TiC/a-C:H nanocomposite and Ti-containing amorphous hydrogenated carbon coatings in reciprocating sliding friction conditions under oil lubrication and at high initial Hertzian contact pressure (1.7 GPa). Under the most severe testing conditions (i.e., high contact pressure, high sliding speed of 100 mm/s, high frequency of 50 Hz), these coatings did not withstand and failure by coating delamination and wear was observed. The authors concluded that a high load-bearing capacity of the coatings is required to withstand such harsh tribological test conditions. This load-bearing capacity is related to hardness and mechanical properties (i.e., Young's modulus), with the volume fraction of (hard) crystalline and (softer, more ductile) amorphous phases, and the ability to form a graphitic-type transfer layer in the contact zone with low shear strength [97]. These conclusions point both towards the technological potential and the challenge of tailoring properties and performance of such carbon-based coatings.

This description of the state-of-the art focuses mainly on mechanical and tribological properties and wear performance of transition metal carbide/amorphous carbon composite thin films in ball-on-disc and oscillating sliding friction experiments, and on the correlation of the thin films' microstructure and constitution and these properties. It should explicitly be mentioned that such materials, in the form of thin films and bulk materials, generally exhibit further interesting physical and chemical properties, making them suitable candidates, for example, for electrical [18,60] and optical applications [63,64,98], medical and biofunctional surfaces [20,59,99,100], electrochemical storage [101,102] and other applications [103]. The opportunity to tune and tailor properties, functionalities and microstructure of such materials will have a huge impact on future materials research, advanced synthesis and utilization, as has been demonstrated recently for magnetron-sputter-deposited TiC/a-C thin films [104–106].

In this work, we present a tribological study on friction and wear performance of a non-reactively magnetron-sputtered hydrogen-free TiC/a-C coating under lubricated reciprocating sliding conditions against 100Cr6 steel. The coating composition has been chosen to be comparable to major work published in the field on unidirectional sliding friction studies in pin-on-disk configurations, and has been set to TiC/a-C 30/70, representing a total carbon content in the range of 75 at.%. Such coatings have been suggested to exhibit optimum friction and wear performance in pin-on-disk testing in various tribosystems [1–5]. The testing conditions realized in the reciprocating sliding friction experiments encompass the utilization of three different lubricant media, as well as variation of the lubricant supply and the normal load during testing. The lubricants are isooctane, ethanol and distilled water, reflecting a recent societal discussion on potential environmentally friendly green technologies in mobility, utilizing new alternative, synthetic or biofuels. The TiC/a-C coating has been chosen as a model thin film material with regard to the already existing knowledge of its materials science and deposition technologies, its technology readiness level and its ability to tailor its microstructure and mechanical and tribological properties over a wide range.

## 2. Materials and Methods

### 2.1. Thin Films

TiC/a-C thin films were deposited by non-reactive D.C. magnetron sputtering in a laboratory-scale commercial PVD unit (Z 550, Leybold GmbH, Cologne, Germany). The sputtering target was an isostatically hot-pressed homogeneous compound target, manufactured from a nominal powder composition of 70 mol.% graphite and 30 mol.% titanium carbide (TiC). Its dimensions were 75 mm diameter, 5 mm thickness, with a mass density above 95%. This target was operated in D.C. power supply mode with a power of 500 W. The deposition processes were carried out with an argon gas pressure of 0.6 Pa (69 sccm argon gas flow). For the thin film samples used in this study, no additional substrate bias was applied (i.e., zero bias, grounded substrates). The target-to-substrate distance was 5 cm. The thickness of the TiC/a-C thin films for the wear tests was adjusted to 5 microns [23,107,108].

Substrate materials used for thin film characterization and wear studies were commercial cemented carbide plates with geometry  $12.5 \times 12.5 \times 4.5 \text{ mm}^3$  (SNUN 120608/401; composition: 88.5 wt.% WC, 11 wt.% Co, 0.5 wt.% Ta-Nb-C; supplier: Walter AG, Tübingen, Germany). The substrate materials were mirror-polished, ultrasonically cleaned for 15 min in acetone and blasted by dry air before being placed in the vacuum chamber. The PVD chamber was pumped to a pressure of  $5 \times 10^{-6}$  mbar. Prior to thin film deposition, the substrates were 15 min plasma-etched in an R.F.-powered argon discharge at a pressure of 0.6 Pa (800 W power, 980 V substrate bias). This pretreatment has been found to be optimum to support thin film adhesion on the substrate samples intended for the wear study. To enhance the adhesion further, a 300 nm thick pure Ti interlayer was deposited before the TiC/a-C thin film deposition. For this purpose, a commercial titanium target (purity 3N5) was used and operated in D.C. mode with power of 500 W, argon gas pressure of 0.6 Pa and 0 V substrate bias. After the deposition of this interlayer, the substrate table was moved to the position of the TiC-C compound target for immediate deposition of the nanocomposite coating without breaking vacuum. Both sputter targets were operated sequentially only, with the use of appropriate shutters.

The TiC/a-C thin films exhibited a Vickers microhardness of 1634 HV<sub>0.05</sub> and showed a critical load of failure,  $L_{CL}$ , in scratch testing of 40 N. Their elemental composition was determined by electron probe micro-analysis (EPMA, Cameca Camebax system, CAMECA, Gennevilliers, France): 23.4 at.% Ti, 75.4 at.% C, 1.2 at.% contamination by Ar, O, N. These values correspond well with the composition of the compound target. Microstructural characterization by means of X-ray diffraction, transmission electron microscopy (cross-sectional dark field imaging, selected area diffraction) and Raman spectroscopy revealed

the coexistence of a nanocrystalline TiC phase with grain size in the range of 5 nm, homogeneously dispersed in an amorphous carbon matrix [23,107,108].

## 2.2. Tribology

The thin films deposited on polished substrates of submicron cemented carbide had a hardness of 1634 HV<sub>0.05</sub> (Figure 1a). In all tribological tests, balls (KGM, Fulda, Germany) with a diameter of 20 mm made of bearing steel 100Cr6 were used as counter bodies. The steel, quenched and tempered to 800 HV, was characterized by a microstructure of tempered martensite and spherical carbides (Figure 1b). 100Cr6 plates with comparable hardness and microstructure (Figure 1c) were used as reference material under all test conditions. In addition, engineering ceramics, namely SiC (EKasic F, ESK Ceramics, Kempten, Germany), Al<sub>2</sub>O<sub>3</sub> (F99.7, Friatec, Mannheim, Germany) and ZrO<sub>2</sub> (ZN101B, Ceramtec, Plochingen, Germany) were included in the investigations under selected conditions. The engineering ceramics showed homogenous microstructures with an average grain size of 1.9 μm (SiC), 7.5 μm (Al<sub>2</sub>O<sub>3</sub>) and 0.3 μm (ZrO<sub>2</sub>) and high hardness of 2540 HV (SiC), 1670 HV (Al<sub>2</sub>O<sub>3</sub>) and 1311 HV (ZrO<sub>2</sub>) (Figure 1d–f).

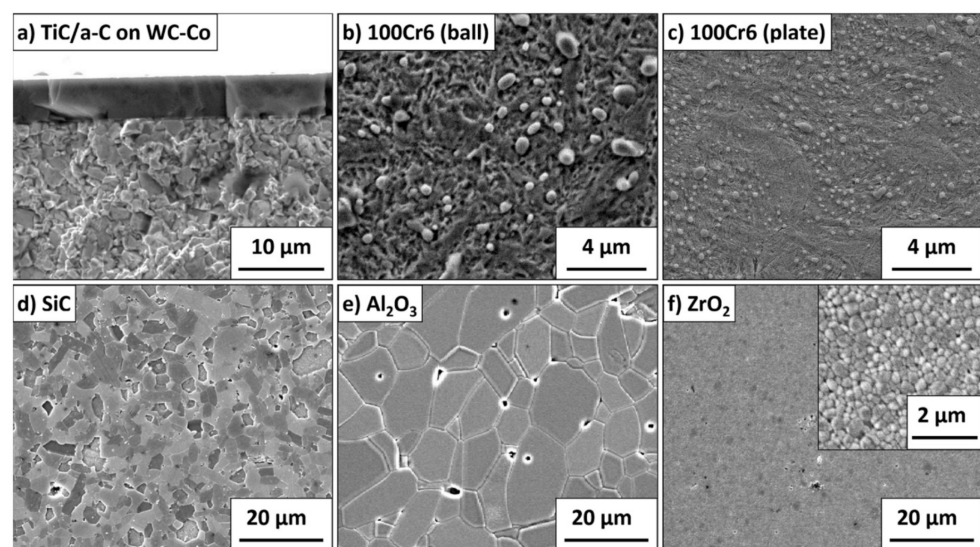


**Figure 1.** SEM micrographs of (a) a cross-sectional view of the TiC/a-C-coated cemented carbide, showing a featureless, homogeneous microstructure of the coating, and cross-sectional views showing the microstructures of (b) 100Cr6 ball, (c) 100Cr6 plate, (d) SiC, (e) Al<sub>2</sub>O<sub>3</sub> and (f) ZrO<sub>2</sub>.

The tribological ball-on-plate tests were run under oscillating sliding conditions in a laboratory tribometer (SRV, Optimol, Munich, Germany) at room temperature, lubricated with isooctane, ethanol or distilled water, as well as unlubricated in ambient atmosphere with a relative humidity of about 50% (Figure 2). The lubricants were selected with regard to the possible use of the materials for tribocomponents in contact with gasoline and alternative biofuels. The liquid media were continuously fed by drip lubrication to ensure continuous immersion of the contact zone. A normal load of 20 N (Hertzian pressure of about 875 MPa for the TiC/a-C thin films), a stroke length of 2.5 mm and a frequency of 20 Hz were chosen as standard conditions, resulting in a total sliding distance of 360 m after 60 min. Additional tests with a normal load that stepwise increased from 20 N up to 160 N were run under lubrication with isooctane. During all tests, the friction force was continuously measured and recorded. Linear wear of the plates  $W_{l,plate}$  was measured after the test using a stylus profilometer (Hommel Ematic T8000 R, Jenoptik, Jena, Germany) and linear wear of the balls  $W_{l,ball}$  was calculated from the diameter of the circular wear scars. All results presented are average values of at least two individual tribological tests.

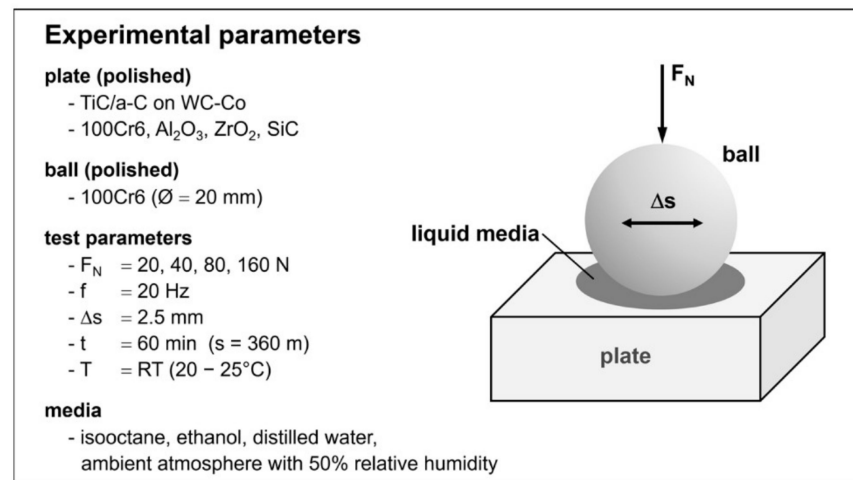


**Figure 2.** Tribological model test setup and experimental parameters.

### 3. Results

The evolution of friction coefficient versus sliding path of all sliding pairs tested under lubrication with isooctane and in unlubricated contact is shown in Figure 3. Lowest friction was measured for TiC/a-C with an average quasi-stationary friction coefficient (last 100 m of sliding path) of about 0.16 for both isooctane lubricated and dry conditions. Lubricated with isooctane bearing steel 100Cr6 showed the highest friction coefficient, with pronounced fluctuations throughout the test and quasi-stationary values of about 0.31. Friction coefficient of the isooctane-lubricated ceramics increased from values of about 0.2 at the very beginning of the tests to quasi-stationary values between 0.24 (SiC) and 0.29 (ZrO<sub>2</sub>). In particular, the pairing of the alumina was characterized by very pronounced fluctuations in the coefficient of friction. Under unlubricated conditions with 50% relative humidity, TiC/a-C was characterized by distinct running-in behavior with friction coefficients up to 1.2 at the very beginning of the test and a sharp decrease to values of about 0.16 after 30 m. Both bearing steel 100Cr6 and the engineering ceramics showed high friction coefficients in dry contact along the entire sliding path with values between 1.0 (100Cr6, SiC, Al<sub>2</sub>O<sub>3</sub>) and 1.25 (ZrO<sub>2</sub>) at the end of the tests.

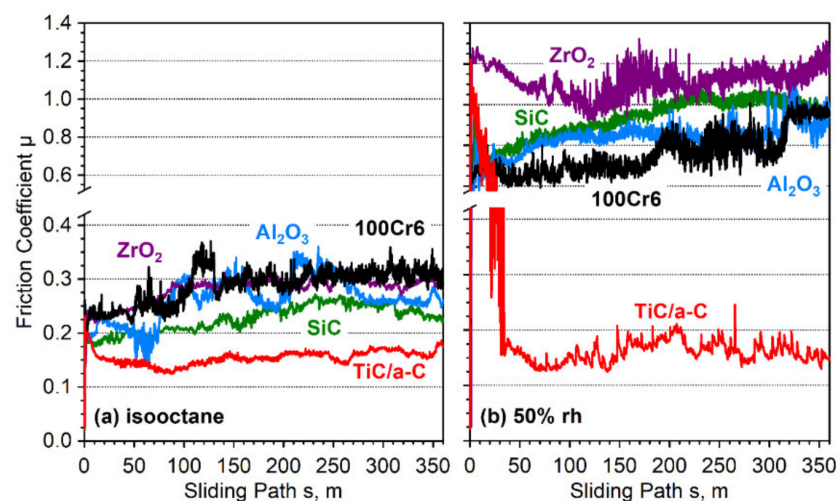


**Figure 3.** Friction coefficient versus sliding path for (a) tests under lubrication with isooctane and (b) unlubricated tests in ambient atmosphere with 50% relative humidity ( $F_N = 20$  N,  $\Delta s = 2.5$  mm,  $f = 20$  Hz, 100Cr6 ball with Ø 20 mm).

The favorable frictional behavior of the TiC/a-C thin film was also reflected in the amount of wear determined after a sliding distance of 360 m, which was about 1  $\mu$ m under

isooctane lubrication and about 2  $\mu\text{m}$  in dry tests, as shown in Figure 4. The wear of the steel ball used as counter body was 2.5 and 5.6  $\mu\text{m}$ , respectively. The engineering ceramics showed an even lower linear wear of less than 1  $\mu\text{m}$  when lubricated with isooctane. However, SiC and  $\text{Al}_2\text{O}_3$  in particular led to significantly higher wear of the steel ball. Therefore, the total wear of the ceramic sliding pairs between 4.2  $\mu\text{m}$  ( $\text{ZrO}_2$ ) and 11.6  $\mu\text{m}$  ( $\text{Al}_2\text{O}_3$ ) was higher than for the TiC/a-C sliding pair (3.6  $\mu\text{m}$ ). Compared to the TiC/a-C nanocomposite, the wear of the 100Cr6 bearing steel was only slightly higher (1.5  $\mu\text{m}$ ), but the wear of the mated ball (10  $\mu\text{m}$ ) was about a factor of three higher than after tests versus TiC/a-C. Under unlubricated conditions, wear of balls and plates of all sliding pairs increased compared to the tests with isooctane lubrication. While the total wear of the pair with the TiC/a-C thin film doubled to about 8  $\mu\text{m}$ , it was about 5 to 8 times higher for the ceramic sliding pairs (33  $\mu\text{m}$  for SiC to 63  $\mu\text{m}$  for  $\text{ZrO}_2$ ) and 15 times higher (85  $\mu\text{m}$ ) for the steel sliding pair.

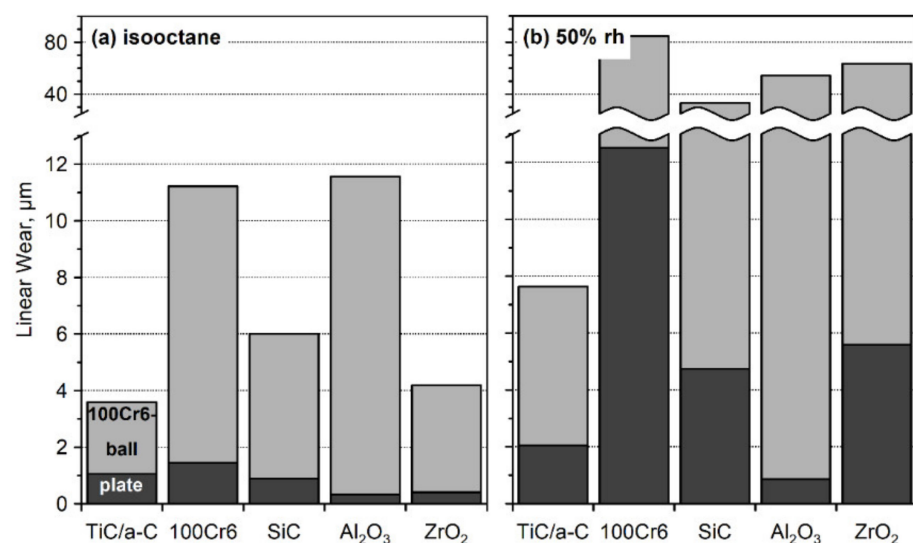


**Figure 4.** Linear wear of plate and ball after a sliding distance of 360 m (a) under lubrication with isooctane and (b) unlubricated in ambient atmosphere with 50% relative humidity ( $F_N = 20$  N,  $\Delta s = 2.5$  mm,  $f = 20$  Hz, 100Cr6 ball with  $\varnothing 20$  mm).

The worn surfaces of plates and balls of the sliding pairs of TiC/a-C thin film, bearing steel and SiC after a sliding distance of 360 m under isooctane lubrication are shown in Figure 5. In good agreement with the relatively low friction coefficients, the surfaces of the plates are very smooth and show only slight grooving (Figure 5a–c). In particular for the steel plate, layers of compacted wear particles are visible on the worn surface (Figure 5b). The surface of the steel ball paired with the TiC/a-C thin film is almost completely covered by a transfer film from the coating (Figure 5d). The surface of the ball running against SiC exhibits not only strongly smoothed areas but also clear grooving due to the very hard counter body (Figure 5f).

After 360 m of sliding in unlubricated contact, both plate and ball surfaces of the steel sliding pair were very rough and were covered by a thick layer of partially compacted wear particles (Figure 6b,e), while the surfaces of the SiC plate and the mated ball were characterized by uniformly grooved surfaces (Figure 6c,f). The TiC/a-C nanocomposite, on the other hand, was very smooth and showed only minimal traces of microabrasion (Figure 6a). A thin, very smooth transfer layer had formed on the mated ball and had also partially detached from the surface (Figure 6d).

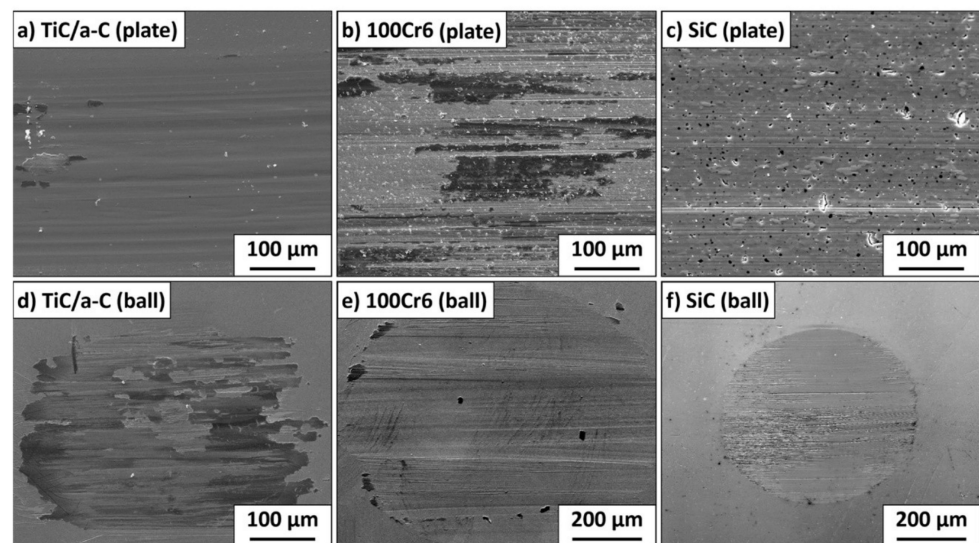


**Figure 5.** SEM images of worn plates (a–c) and balls (d–f) after a sliding distance of 360 m under lubrication with isooctane: (a,d) 100Cr6 sliding pair and (b,e) TiC/a-C sliding pair and (c,f) SiC sliding pair ( $F_N = 20$  N,  $\Delta s = 2.5$  mm,  $f = 20$  Hz, 100Cr6 ball with  $\varnothing 20$  mm).

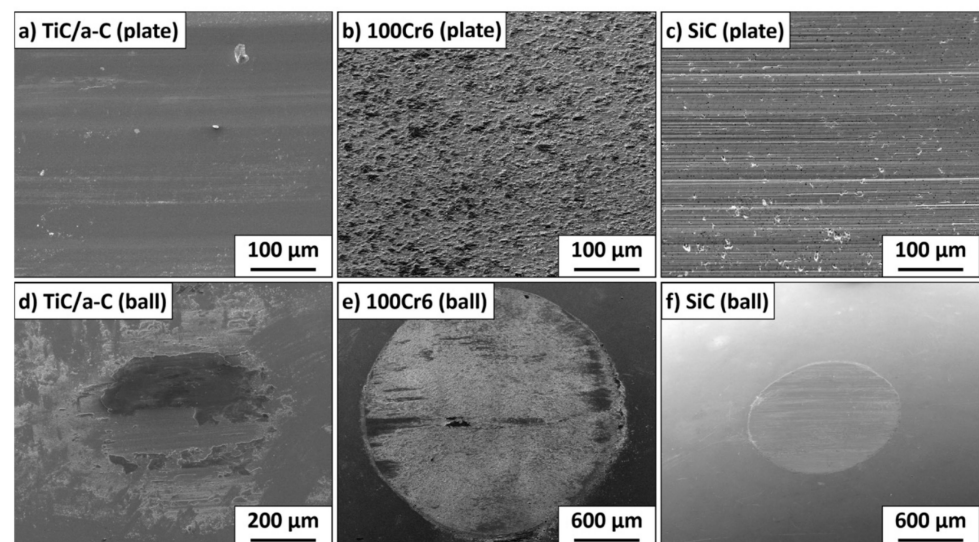


**Figure 6.** SEM images of worn plates (a–c) and balls (d–f) after a sliding distance of 360 m in ambient air with 50% relative humidity: (a,d) 100Cr6 sliding pair and (b,e) TiC/a-C sliding pair and (c,f) SiC sliding pair ( $F_N = 20$  N,  $\Delta s = 2.5$  mm,  $f = 20$  Hz, 100Cr6 ball with  $\varnothing 20$  mm).

The influence of the stepwise increased normal load on friction of TiC/a-C and steel 100Cr6 under lubrication with isooctane is shown in Figure 7a. Friction coefficient of the TiC/a-C sliding pair decreased with increasing normal load from values of about 0.2 at the beginning of the tests and a normal load of 20 N to a final value of 0.11 for 160 N at the end of the test. In contrast, the coefficient of friction for the self-mated steel 100Cr6 increased from values of around 0.3 to values around 0.8 as the normal load was increased from 20 to 40 N. After a further increase in the normal load to 80 N, the test had to be stopped due to a sharp increase in the coefficient of friction and galling in the contact zone. The linear wear of the steel pairing after a sliding distance of 720 m was 15  $\mu\text{m}$  for the plate and 31  $\mu\text{m}$  for the ball (Figure 7b). Despite the higher load and a twice as long sliding distance of 1440 m, the TiC/a-C thin film showed linear wear of only 3.8  $\mu\text{m}$  at the end of the test. The wear of the steel ball was 6.4  $\mu\text{m}$  for the TiC/a-C sliding pair.

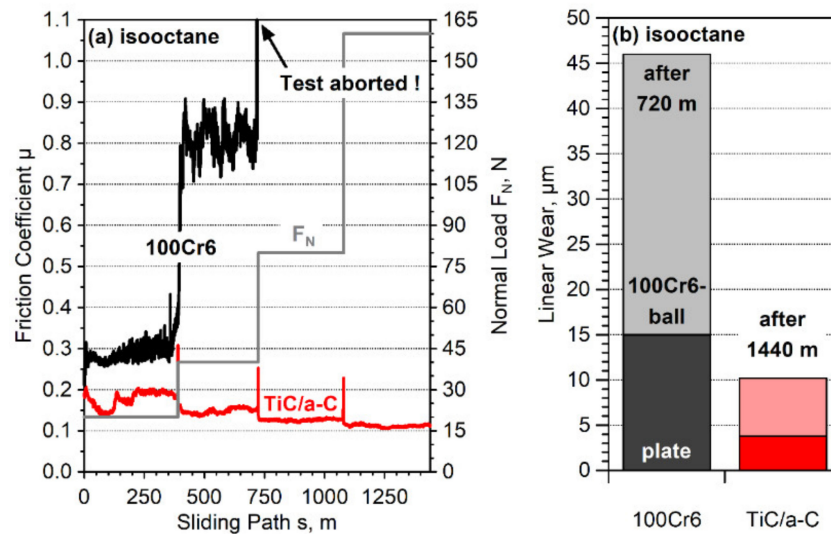


**Figure 7.** (a) Friction coefficient versus sliding path for tests under lubrication with isooctane and stepwise increased normal load and (b) linear wear of plate and ball after tests of TiC/a-C and steel 100Cr6 ( $F_N = 20/40/80/160$  N,  $\Delta s = 2.5$  mm,  $f = 20$  Hz, 100Cr6 ball with  $\varnothing 20$  mm).

With regard to a possible use in biofuel applications, the tribological performance of TiC/a-C nanocomposite thin film and bearing steel 100Cr6 was additionally characterized under lubrication with ethanol and distilled water (Figure 8). The TiC/a-C nanocomposite thin film sliding pairs showed a quasi-stationary coefficient of friction below 0.2 for all test conditions. For tests with ethanol and distilled water, the final friction coefficient of 0.14 was somewhat lower than for lubrication with isooctane (Figure 8a). A significant influence of the interfacial medium on friction was observed for the steel sliding pair (Figure 8b). Under water lubrication, the coefficient of friction of around 0.45 at the end of the test was about 50% higher than that under isooctane lubrication. The lowest friction coefficient slightly below 0.2 was observed for the self-mated steel when lubricated with ethanol. Comparable to the TiC/a-C sliding pair, the self-mated steel showed the lowest fluctuations in the friction coefficient under ethanol lubrication.

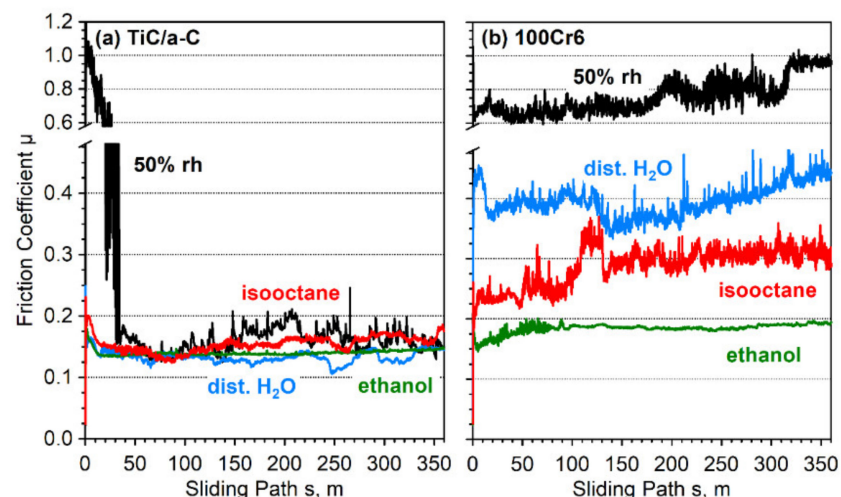


**Figure 8.** Friction coefficient versus sliding path for (a) tests under lubrication with isooctane and (b) unlubricated tests of TiC/a-C and steel 100Cr6 in air with 50% rh ( $F_N = 20$  N,  $\Delta s = 2.5$  mm,  $f = 20$  Hz, 100Cr6 ball with  $\varnothing 20$  mm).

For both sliding pairs, the lowest total wear was found when lubricated with ethanol (Figure 9). For the steel sliding pair, the total linear wear of 6  $\mu\text{m}$  was about half of that under isooctane lubrication (Figure 9b). The linear wear of the TiC/a-C thin film was

almost unmeasurable, with less than 0.1  $\mu\text{m}$  in ethanol, and the total wear of the sliding pair was below 3  $\mu\text{m}$  (Figure 9a). Distilled water resulted in a significant increase in linear wear of the plates to values of about 3  $\mu\text{m}$  (100Cr6) and 4  $\mu\text{m}$  (TiC/a-C) in both pairings compared to isooctane. For the TiC/a-C thin film, the wear under water lubrication was about twice as high as under unlubricated conditions.

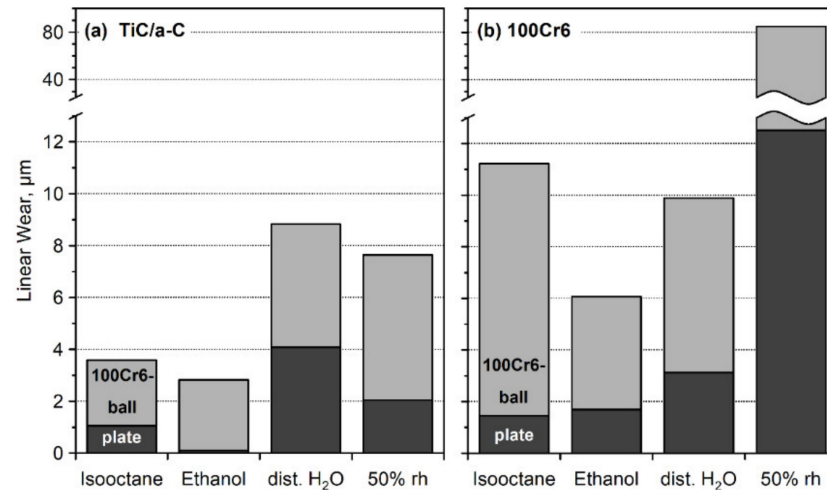


**Figure 9.** Linear wear of plate and ball after a sliding distance of 360 m lubricated with isooctane, ethanol or distilled water and unlubricated in ambient atmosphere with 50% rh for (a) bearing steel 100Cr6 and (b) TiC/a-C coating ( $F_N = 20\text{ N}$ ,  $\Delta s = 2.5\text{ mm}$ ,  $f = 20\text{ Hz}$ , 100Cr6 ball with  $\text{Ø} 20\text{ mm}$ ).

Worn surfaces after the tests under ethanol lubrication are shown in Figure 10. No significant wear-related alterations were observed on the TiC/a-C thin film apart from further smoothing (Figure 10a). Rather, original topographic features of the deposited layers are still very clearly visible (Figure 10b). The steel ball of the TiC/a-C sliding pair exhibits a smoothed surface with some scratching (Figure 10c). The worn surfaces of the 100Cr6 steel plate and ball are both characterized by grooving parallel to the sliding direction and a pronounced relief-like surface topography (Figure 10d–f), which indicates a selective corrosion attack.

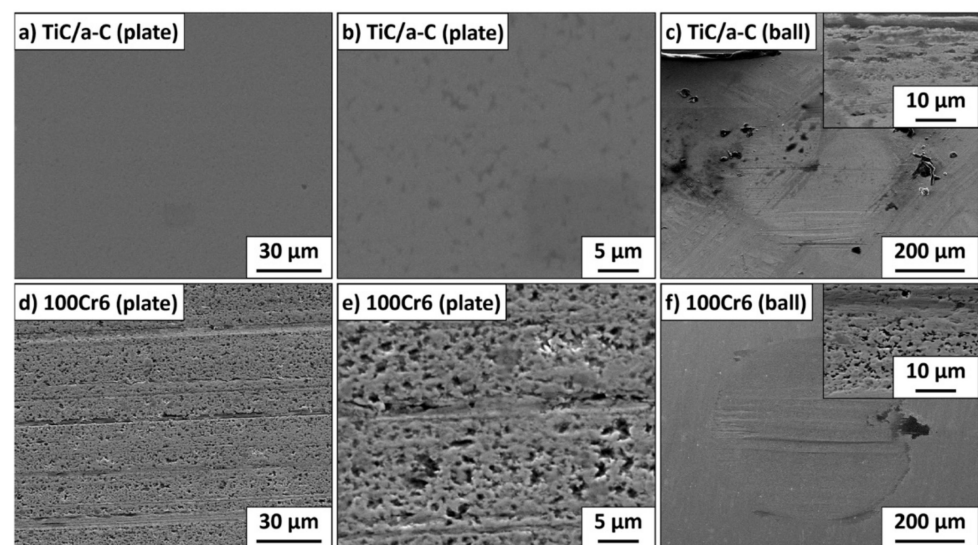


**Figure 10.** SEM images of worn plates (a,b,d,e) and balls (c,f) after a sliding distance of 360 m under lubrication with ethanol: (a–c) 100Cr6 sliding pair and (d–f) TiC/a-C sliding pair ( $F_N = 20\text{ N}$ ,  $\Delta s = 2.5\text{ mm}$ ,  $f = 20\text{ Hz}$ ).

After tests under water lubrication, the TiC/a-C thin film was characterized by macroscopically uneven material removal and a microscopically extremely smoothed surface without any scratches (Figure 11a,b). The 100Cr6 ball was partially covered by a layer; build up from compacted debris and transferred material from the thin film (Figure 11c). Worn surfaces of both steel plate and ball show fine scratching along the sliding direction (Figure 11d–f). In particular, the worn surface of the steel ball is largely covered by a layer of finely ground and compacted wear particles (Figure 11f).

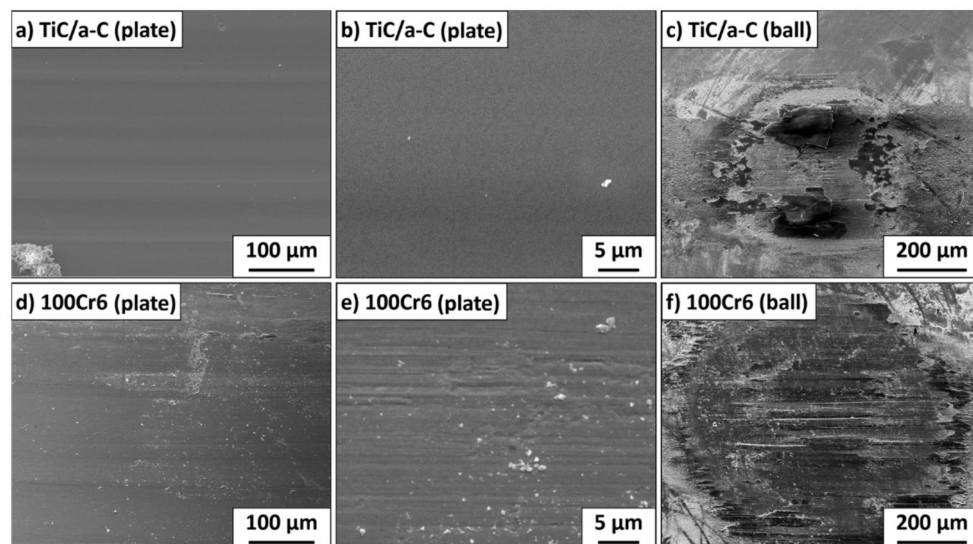


**Figure 11.** SEM images of worn plates (a,b,d,e) and balls (c,f) after a sliding distance of 360 m under lubrication with distilled water: (a–c) 100Cr6 sliding pair and (d–f) TiC/a-C sliding pair ( $F_N = 20$  N,  $\Delta s = 2.5$  mm,  $f = 20$  Hz).

#### 4. Discussion

TiC/a-C nanocomposite thin films with an amount of about 75 at.% of carbon were tribologically characterized under oscillating sliding conditions in contact with a 100Cr6 steel ball. In a first step, the tribological performance of the thin film was compared to steel 100Cr6 and engineering ceramics SiC, Al<sub>2</sub>O<sub>3</sub> and ZrO<sub>2</sub>. The TiC/a-C sliding pair showed the lowest friction both under unlubricated conditions in ambient atmosphere with 50% relative humidity and in the mixed lubrication regime with isooctane. The quasi-stationary friction coefficient of about 0.16 for TiC/a-C under both conditions could be attributed to the formation of a transfer layer on the steel ball (see Figures 5d and 6d), which determined the friction behavior in the further course of the tests. This favorable behavior is described in the literature for both DLC and various MeC/a-C thin films (e.g., [3,6,8,77,109]). The values determined for the coefficient of friction of the TiC/a-C thin films in this study are significantly higher than typical values of less than 0.1 often published for tests of comparable thin films under unlubricated sliding conditions. This can be attributed to the fact that the investigations presented here were carried out under much less favorable oscillating conditions and not under unidirectional sliding conditions.

The low-viscosity isooctane did not significantly reduce the friction coefficient, but had a positive effect on the running-in behavior at the beginning of the test, since it reduced the proportion of solid/solid contacts, causing increased friction in the unlubricated sliding couple during the first approximately 30 m of sliding distance until the surface of the thin film was smoothed and a stable transfer layer was built up (see Figure 3a,b). As a result, wear was about halved compared to the unlubricated contact. The effective formation of the transfer layer could also be illustrated by an additional experiment in which the supply of isooctane was stopped after a sliding distance of 30 m (Figure 12). For the 100Cr6 reference sliding pair, this led to an abrupt increase in the friction coefficient after the isooctane had evaporated and a transition from the mixed lubrication regime to the adhesion-controlled

high friction and wear regime at a sliding distance of about 150 m. In contrast, the friction coefficient for the TiC/a-C sliding pair decreased continuously in the further course of the test. When lubricated with isooctane, the engineering ceramics consistently showed a significantly higher coefficient of friction compared to the TiC/a-C thin film, but also slightly lower wear. While in the pairing with TiC/a-C, the formation of a transfer layer associated with a transfer from the thin film to the steel ball led not only to a reduction in friction but also to wear protection of the steel ball, such transfer layer formation was not observed on the steel balls paired with the ceramics. Here, the hard ceramic surfaces led to pronounced abrasive wear on the steel balls (see Figure 5f). The highest wear occurred for the pairing with the Al<sub>2</sub>O<sub>3</sub> ceramic, which is attributed to the increased roughness of the initial surface compared to the other two ceramics. Despite their significantly higher hardness compared to the 100Cr6 steel, SiC and ZrO<sub>2</sub> resulted in less wear on the steel ball. This can be attributed to the reduced adhesion tendency of the ceramic/metal pairings compared to the metal/metal pairing. Under unlubricated conditions, the high friction coefficients typical of metal/ceramic pairings led to an increase in wear on both the ceramic plates and the steel balls in particular [110,111]. Compared to Al<sub>2</sub>O<sub>3</sub> and ZrO<sub>2</sub>, the significantly harder SiC plate exhibited higher wear both in unlubricated contact and under lubrication with isooctane. In [112], tribological investigations of SiC under unlubricated sliding conditions with various steels revealed the unfavorable influence of the alloying element Cr, which favors tribochemical attack of SiC through the formation of chromium oxides, which, for example, were successfully used for tribochemical polishing of SiC and Si<sub>3</sub>N<sub>4</sub> ceramics [113,114]. The very smooth SiC surfaces with fine scratches at the end of the test are a further illustration of this effect (see Figures 5c and 6c).

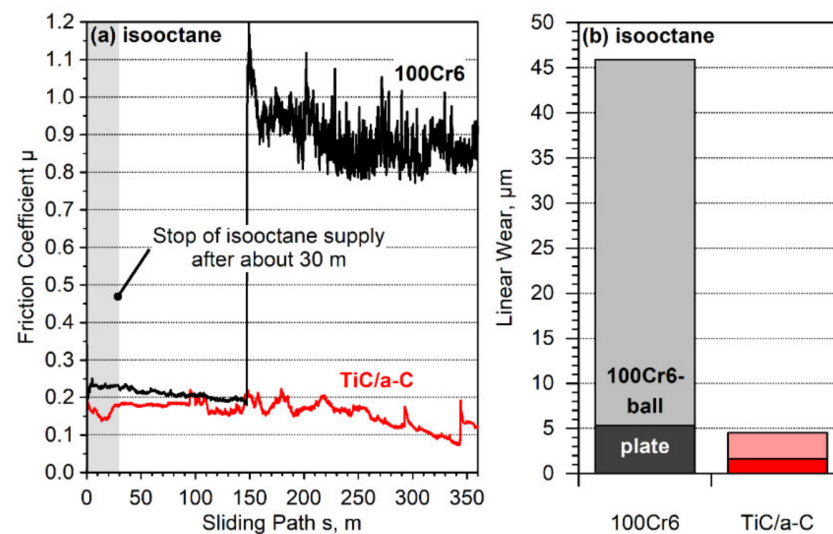


**Figure 12.** (a) Friction coefficient versus sliding path and (b) linear wear of plate and ball after a sliding distance of 360 m for tests of TiC/a-C and steel 100Cr6 during which the supply with isooctane was stopped after a sliding distance of 30 m and the remaining tests were run without further lubrication ( $F_N = 20/40/80/160$  N,  $\Delta s = 2.5$  mm,  $f = 20$  Hz, 100Cr6 ball with  $\varnothing 20$  mm).

Further investigations on the influence of the lubricant on the friction and wear behavior of the TiC/a-C thin film were carried out using the self-mated steel as a reference. All three liquid media used for lubrication were characterized by low viscosity. At 20 °C, ethanol (1.26 mPas) had slightly higher dynamic viscosity than water (1.02 mPas), while isooctane had the lowest value of only 0.5 mPas. Looking at the results of the tribological model tests (Figure 8a), the differences in viscosity of the three lubricating media do not appear to play a significant role in the friction of the TiC/a-C thin films. This can be attributed to the fact that friction of the sliding couples with the TiC/a-C thin films was largely determined by the material transfer to the steel ball and the following self-lubrication effect. These transfer films were found on the steel balls after the tests with

TiC/a-C for all tested conditions (Figures 5d, 6d, 10c and 11c). In contrast to the TiC/a-C couples, the self-paired steel showed a very clear influence of the lubricating media on the frictional behavior under the prevailing mixed lubrication conditions. However, the magnitude of the measured friction coefficient did not correlate with viscosity here either. The highest friction coefficient was observed for lubrication with water and the lowest for lubrication with ethanol. This indicates that tribochemical interactions between the media and the mated steel surfaces may play a decisive role. Isooctane, which has the lowest viscosity of the lubricants used, but at the same time as a non-polar liquid in contrast to the highly polar-distilled water, did not lead to any significant tribochemical interaction with the steel surface, and thus favored the formation of very smooth surfaces (Figure 5b,e). Under water lubrication, on the other hand, thick layers of compacted, mainly oxidic wear particles were formed due to the corrosive attack of the steel surfaces, especially on the steel balls, which were in contact over the entire test duration (Figure 11d–f). This can explain the lower friction under isooctane lubrication. The very low friction coefficient of the steel pairing under ethanol lubrication can be traced back to the in situ forming surface topography in the contact zone with a high material ratio and simultaneously sufficient lubricant reservoirs (Figure 10d–f). This topography was formed as a result of a less pronounced, selective corrosion attack by the ethanol compared to water, which was also observed in other tribological investigations of steel pairings in ethanol or ethanol-containing media [115,116]. The observed friction-reducing surface topographies are similar to those produced by adapted finishing (e.g., honing and subsequent chemical etching) of AlSi cylinder bore surfaces [117] or by laser surface texturing [118].

While the three lubricating media had no significant effect on the frictional behavior of the TiC/a-C thin films, they certainly influenced the wear behavior of the coatings. The highest wear was measured after tests in water. This, together with the microscopically very smooth surfaces of the thin films after the end of the experiments, suggests a tribochemical wear mechanism triggered by the strongly polar water molecules. This observation is consistent with the fact that the reactive hydroxyl group (-OH) constitutes almost the entire water molecule, while in ethanol it forms only a minor part of the molecule ( $\text{CH}_3\text{-CH}_2\text{-OH}$ ) and hence there is a less severe triboreaction. Accordingly, the interactions were also more pronounced under water lubrication than in moist air, so that less wear was measured in the unlubricated tests in ambient atmosphere with 50% relative humidity than under water lubrication. Under the conditions of oscillating sliding contact chosen in this study, the formation of a stable tribochemical reaction layer is clearly more difficult than in unidirectional sliding contact, which can explain not only the higher friction but also the increased wear compared to other studies [119,120]. On the other side, the lowest wear of the TiC/a-C thin film was not found for the tests with the non-polar isooctane but for the hygroscopic ethanol. Besides viscosity and polarity of the liquid media, further influencing factors must be considered. One might argue that the ethanol's OH group may interact with the polar surfaces of metals and metal oxides, leaving the non-polar ethyl end ( $\text{CH}_3\text{-CH}_2\text{-}$ ) in the direction of the friction counterpart. In this way, it may protect the underlying solid surface and may even favor the formation of bilayers, which would mediate friction forces by shearing displacement of such bilayers with respect to each other. No interactions of this type are possible in isooctane, and hence its lubricating action is not as efficient as that of ethanol. The corrosive attack of the surfaces observed for the steel self-pairing did not occur to this extent for the steel ball in pairing with TiC/a-C. Quite obviously, a sufficient passivation of the steel surface was already achieved by the very low removal and transfer from the TiC/a-C thin film, which reduced further wear. However, within the framework of this study, the effective mechanisms could not yet be fully elucidated, so further investigations are planned.

**Author Contributions:** Conceptualization, methodology, investigation, data curation, formal analysis, supervision, project administration, resources, J.S. and M.S.; writing—original draft preparation, J.S. and M.S.; validation, visualization, writing—review and editing, J.S., S.U., J.P. and M.S. All authors have read and agreed to the published version of the manuscript.

**Funding:** This research received no external funding.

**Institutional Review Board Statement:** Not applicable.

**Informed Consent Statement:** Not applicable.

**Data Availability Statement:** All data are contained within the article. Further, the data presented in this study are available on request from the corresponding authors.

**Acknowledgments:** The authors would like to express their sincere thanks to Katja Hahn for the scanning electron microscopic investigations on the specimens. We further acknowledge support by the KIT-Publication Fund of the Karlsruhe Institute of Technology.

**Conflicts of Interest:** The authors declare no conflict of interest.

## References

1. Voevodin, A.A.; Prasad, S.V.; Zabinski, J.S. Nanocrystalline carbide/amorphous carbon composites. *J. Appl. Phys.* **1997**, *82*, 855–858. [[CrossRef](#)]
2. Zehnder, T.; Patscheider, J. Nanocomposite TiC/a-C:H hard coatings deposited by reactive PVD. *Surf. Coat. Technol.* **2000**, *133–134*, 138–144. [[CrossRef](#)]
3. Pei, Y.T.; Galvan, D.; De Hosson, J.T.M.; Cavaleiro, A. Nanostructured TiC/a-C coatings for low friction and wear resistant applications. *Surf. Coat. Technol.* **2005**, *198*, 44–50. [[CrossRef](#)]
4. Martínez-Martínez, D.; López-Cartes, C.; Fernández, A.; Sánchez-López, J.C. Comparative performance of nanocomposite coatings of TiC or TiN dispersed in a-C matrixes. *Surf. Coat. Technol.* **2008**, *203*, 756–760. [[CrossRef](#)]
5. Musil, J.; Novák, P.; Cerstvý, R.; Soukup, Z. Tribological and mechanical properties of nanocrystalline TiC/a-C nanocomposite thin films. *J. Vac. Sci. Technol. A* **2010**, *28*, 244–249. [[CrossRef](#)]
6. Soucek, P.; Schmidtová, T.; Bursikova, V.; Vasina, P.; Pei, Y.T.; De Hosson, J.T.M.; Caha, O.; Perina, V.; Miksova, R.; Malinsky, P. Tribological properties of nc-TiC/a-C:H coatings prepared by magnetron sputtering at low and high ion bombardment of the growing film. *Surf. Coat. Technol.* **2014**, *241*, 64–73. [[CrossRef](#)]
7. Jiang, X.; Yang, F.-C.; Lee, J.-W.; Chang, C.-L. Effect of an optical emission spectrometer feedback-controlled method on the characterizations of nc-TiC/a-C:H coated by high power impulse magnetron sputtering. *Diam. Relat. Mater.* **2017**, *73*, 19–24. [[CrossRef](#)]
8. Sánchez-López, J.C.; Dominguez-Meister, S.; Rojas, T.C.; Colasuonno, M.; Bazzan, M.; Patelli, A. Tribological properties of TiC/a-C:H nanocomposite coatings prepared by HIPIMS. *Appl. Surf. Sci.* **2018**, *440*, 458–466. [[CrossRef](#)]
9. Hauert, R.; Patscheider, J. From alloying to nanocomposites—Improved performance of hard coatings. *Adv. Eng. Mater.* **2000**, *2*, 247–259. [[CrossRef](#)]
10. Patscheider, J.; Zehnder, T.; Diserens, M. Structure-property relations in nanocomposite coatings. *Surf. Coat. Technol.* **2001**, *146–147*, 201–208. [[CrossRef](#)]
11. Pei, Y.T.; Galvan, D.; De Hosson, J.T.M. Nanostructure and properties of TiC/a-C:H composite coatings. *Acta Mater.* **2005**, *53*, 4505–4521. [[CrossRef](#)]
12. Sánchez-López, J.C.; Martínez-Martínez, D.; López-Cartes, C.; Fernández, A. Tribological behavior of titanium carbide/amorphous carbon nanocomposite coatings: From macro to the micro-scale. *Surf. Coat. Technol.* **2008**, *202*, 4011–4018. [[CrossRef](#)]
13. Jansson, U.; Lewin, E.; Rasander, M.; Eriksson, O.; André, B.; Wiklund, U. Design of carbide-based nanocomposite thin films by selective alloying. *Surf. Coat. Technol.* **2011**, *206*, 583–590. [[CrossRef](#)]
14. Jansson, U.; Lewin, E. Sputter deposition of transition-metal carbide films—A critical review from a chemical perspective. *Thin Solid Film.* **2013**, *536*, 1–24. [[CrossRef](#)]
15. Larhlimi, H.; Ghailane, A.; Makha, M.; Alami, J. Magnetron sputtered titanium carbide-based coatings: A review of science and technology. *Vacuum* **2022**, *197*, 110853. [[CrossRef](#)]
16. Feng, B.; Cao, D.M.; Meng, W.J.; Xu, J.; Tittsworth, R.C.; Rehn, L.E.; Baldo, P.M.; Doll, G.L. Characterization of microstructure and mechanical behavior of sputter deposited Ti-containing amorphous carbon coatings. *Surf. Coat. Technol.* **2001**, *148*, 153–162. [[CrossRef](#)]
17. Zhang, S.; Bui, X.L.; Jiang, J.; Li, X. Microstructure and tribological properties of magnetron-sputtered nc-TiC/a-C nanocomposite. *Surf. Coat. Technol.* **2005**, *198*, 206–211. [[CrossRef](#)]
18. Lewin, E.; Wilhelmsson, O.; Jansson, U. Nanocomposite nc-TiC/a-C thin films for electrical contact applications. *J. Appl. Phys.* **2006**, *100*, 054303. [[CrossRef](#)]
19. Moskalewicz, T.; Wendler, B.; Czyska-Filemonowicz, A. Microstructural characterization of nanocomposite nc-MeC/a-C coatings on oxygen hardened Ti-6Al-4V alloy. *Mater. Charact.* **2010**, *61*, 959–968. [[CrossRef](#)]
20. Balászi, K.; Vandrovcová, M.; Bacaková, L.; Balászi, C. Structural and biocompatible characterization of TiC/a:C nanocomposite thin films. *Mater. Sci. Eng. C* **2013**, *33*, 1671–1675. [[CrossRef](#)]
21. Sánchez-López, J.C.; Martínez-Martínez, D.; Abad, M.D.; Fernández, A. Metal carbide/amorphous C-based nanocomposite coatings for tribological applications. *Surf. Coat. Technol.* **2009**, *204*, 947–954. [[CrossRef](#)]
22. Glechner, T.; Hahn, R.; Zauner, L.; Rišlegger, S.; Kirnbauer, A.; Polcik, P.; Riedl, H. Structure and mechanical properties of reactive and non-reactive sputter deposited WC based coatings. *J. Alloy. Compd.* **2021**, *885*, 161129. [[CrossRef](#)]

23. Stüber, M.; Leiste, H.; Ulrich, S.; Holleck, H.; Schild, D. Microstructure and properties of low friction TiC-C nanocomposite coatings deposited by magnetron sputtering. *Surf. Coat. Technol.* **2002**, *150*, 218–226. [[CrossRef](#)]
24. Hu, Y.; Li, L.; Cai, X.; Chen, Q.; Chu, P.K. Mechanical and tribological properties of TiC/amorphous hydrogenated carbon composite coatings fabricated by DC magnetron sputtering with and without sample bias. *Diam. Relat. Mater.* **2007**, *16*, 181–186. [[CrossRef](#)]
25. Polcar, T.; Vitu, T.; Cvrcek, L.; Novak, R.; Vyskocil, J.; Cavaleiro, A. Tribological behaviour of nanostructured Ti-C:H coatings for biomedical applications. *Solid State Sci.* **2009**, *11*, 1757–1761. [[CrossRef](#)]
26. Soucek, P.; Schmidtová, T.; Zábbransky, L.; Bursikova, V.; Vasina, P.; Caha, O.; Jilek, M.; El Mel, A.; Tessier, P.-Y.; Schäfer, J.; et al. Evaluation of composition, mechanical properties and structure of nc-TiC/a-C:H coatings prepared by balanced magnetron sputtering. *Surf. Coat. Technol.* **2012**, *211*, 111–116. [[CrossRef](#)]
27. Makowka, M.; Pawlak, W.; Konarski, P.; Wendler, B. Hydrogen content influence on tribological properties of nc-WC/a-C:H coatings. *Diam. Relat. Mater.* **2016**, *67*, 16–25. [[CrossRef](#)]
28. Singh, V.; Jiang, J.C.; Meletis, E.I. Cr-diamondlike carbon nanocomposite thin films: Synthesis, characterization and properties. *Thin Solid Film.* **2005**, *489*, 150–158. [[CrossRef](#)]
29. Gassner, G.; Patscheider, J.; Mayrhofer, P.H.; Hegedus, E.; Tóth, L.; Kovacs, I.; Pécz, B.; Srot, V.; Scheu, C.; Mitterer, C. Structure of sputtered nanocomposite CrC<sub>x</sub>/a-C:H thin films. *J. Vac. Sci. Technol. B Microelectron. Nanometer Struct. Processing Meas. Phenom.* **2006**, *24*, 1837–1843. [[CrossRef](#)]
30. Keunecke, M.; Bewilogua, K.; Becker, J.; Gies, A.; Grischke, M. CrC/a-C:H coatings for highly loaded, low friction applications under formulated oil lubrication. *Surf. Coat. Technol.* **2012**, *207*, 270–278. [[CrossRef](#)]
31. Meng, W.J.; Tittsworth, R.C.; Rehn, L.E. Mechanical properties and microstructure of TiC/amorphous hydrocarbon nanocomposite coatings. *Thin Solid Film.* **2000**, *377–378*, 222–232. [[CrossRef](#)]
32. Voevodin, A.A.; O'Neill, J.P.; Prasad, S.V.; Zabinski, J.S. Nanocrystalline WC and WC/a-C composite coatings produced from intersected plasma fluxes at low deposition temperature. *J. Vac. Sci. Technol. A* **1999**, *17*, 986–992. [[CrossRef](#)]
33. Zhou, Z.; Rainforth, W.M.; Gass, M.H.; Bleloch, A.; Ehiassarian, A.P.; Hovsepian, P.E. C/CrC nanocomposite coating deposited by magnetron sputtering at high ion irradiation conditions. *J. Appl. Phys.* **2011**, *110*, 073301. [[CrossRef](#)]
34. Makówka, M.; Pawlak, W.; Konarski, P.; Wendler, B.; Szymanowski, H. Modification of magnetron sputter deposition of nc-WC/a-C(:H) coatings with an additional RF discharge. *Diam. Relat. Mater.* **2019**, *98*, 107509. [[CrossRef](#)]
35. Coronel, E.; Wiklund, U.; Olsson, E. The effect of carbon content on the microstructure of hydrogen-free physical vapour deposited titanium carbide films. *Thin Solid Film.* **2009**, *518*, 71–76. [[CrossRef](#)]
36. Pei, Y.T.; Chen, C.Q.; Shaha, K.P.; De Hosson, J.Th.M.; Bradley, J.W.; Voronin, S.A.; Cada, M. Microstructural control of TiC/a-C nanocomposite coatings with pulsed magnetron sputtering. *Acta Mater.* **2008**, *56*, 696–709. [[CrossRef](#)]
37. Precht, W.; Czyzniewski, A. Deposition and some properties of carbide/amorphous carbon nanocomposites for tribological application. *Surf. Coat. Technol.* **2003**, *174–175*, 979–983. [[CrossRef](#)]
38. Lin, J.; Moore, J.J.; Mishra, B.; Pinkas, M.; Sproul, W.D. Syntheses and characterization of TiC/a:C composite coatings using pulsed closed field unbalanced magnetron sputtering (P-CFUBMS). *Thin Solid Film.* **2008**, *517*, 1131–1135. [[CrossRef](#)]
39. Gulbinski, W.; Mathur, S.; Shen, H.; Suszko, T.; Gilewicz, A.; Warcholinski, B. Evaluation of phase, composition, microstructure and properties in TiC/a-C:H thin films deposited by magnetron sputtering. *Appl. Surf. Sci.* **2005**, *239*, 302–310. [[CrossRef](#)]
40. Shaha, K.P.; Pei, Y.T.; Martinez-Martinez, D.; Sanchez-Lopez, J.C.; De Hosson, J.T.M. Effect of process parameters on mechanical and tribological performance of pulsed-DC sputtered TiC/a-C:H nanocomposite films. *Surf. Coat. Technol.* **2010**, *205*, 2633–2642. [[CrossRef](#)]
41. Samuelsson, M.; Sarakinos, K.; Högberg, H.; Lewin, E.; Jansson, U.; Wälivaara, B.; Ljungcrantz, H.; Helmersson, U. Growth of Ti-C nanocomposite films by reactive high power impulse magnetron sputtering under industrial conditions. *Surf. Coat. Technol.* **2012**, *206*, 2396–2402. [[CrossRef](#)]
42. Soucek, P.; Daniel, J.; Hnilica, J.; Bernátova, K.; Zábbransky, L.; Bursikova, V.; Stupavski, M.; Vasina, P. Superhard nanocomposite nc-TiC/a-C:H coatings: The effect of HIPIMS on coating microstructure and mechanical properties. *Surf. Coat. Technol.* **2017**, *311*, 257–267. [[CrossRef](#)]
43. Lou, B.-S.; Hsiao, Y.-T.; Chang, L.-C.; Diyatmika, W.; Lee, J.-W. The influence of different power supply modes on the microstructure, mechanical, and corrosion properties of nc-TiC/a-C:H nanocomposite coatings. *Surf. Coat. Technol.* **2021**, *422*, 127512. [[CrossRef](#)]
44. Evaristo, M.; Fernandes, F.; Cavaleiro, A. Room and high temperature tribological behaviour of W-DLC coatings produced by DCMS and hybrid DCMS-HIPIMS configuration. *Coatings* **2020**, *10*, 319. [[CrossRef](#)]
45. Wang, Y.; Zhang, X.; Wu, X.; Zhang, H.; Zhang, X. Superhard nanocomposite nc-TiC/a-C:H film fabricated by filtered cathodic vacuum arc technique. *Appl. Surf. Sci.* **2008**, *254*, 5085–5088. [[CrossRef](#)]
46. Zhai, Y.-H.; Zhang, Y.-J.; Peng, Y.; Zhang, S.-M.; Zhang, P.-Y.; Zhang, X.-M. Structure and mechanical properties of nc-TiC/a-C:H nanocomposite films deposited by filtered cathodic arc technique. *Rare Met.* **2016**, *35*, 177–183. [[CrossRef](#)]
47. Luo, J.; Zhang, Z.Q.; Pang, P.; Chen, L.; Liao, B.; Shang, H.Z.; Zhang, X.; Wu, X.Y. Low friction coefficient of superhard nc-TiC/a-C:H nanocomposite coatings deposited by filtered cathodic vacuum arc. *Mater. Res. Express* **2019**, *6*, 096418. [[CrossRef](#)]
48. Strondl, C.; Carvalho, N.M.; De Hosson, J.Th.M.; van der Kolk, G.J. Investigation on the formation of tungsten carbide in tungsten-containing diamond like carbon coatings. *Surf. Coat. Technol.* **2003**, *162*, 288–293. [[CrossRef](#)]
49. Abad, M.D.; Munoz-Marquez, M.A.; El Mrabet, S.; Justo, A.; Sánchez-López, J.C. Tailored synthesis of nanostructured WC/a-C coatings by dual magnetron sputtering. *Surf. Coat. Technol.* **2010**, *204*, 3490–3500. [[CrossRef](#)]

50. Drábik, M.; Truchlý, M.; Ballo, V.; Roch, T.; Kvetková, L.; Kús, P. Influence of substrate material and its plasma pretreatment on adhesion and properties of WC/a-C:H nanocomposite coatings deposited at low temperature. *Surf. Coat. Technol.* **2018**, *333*, 138–147. [[CrossRef](#)]
51. Chang, C.-L.; Yang, F.-C.; Chang, T.-M.; Hwang, J.-J. Effect of insert mid-frequency pulses on I-V characterisation, deposition rates and properties of nc-WC/a-C:H films prepared by superimposed HIPIMS process. *Surf. Coat. Technol.* **2018**, *350*, 977–984. [[CrossRef](#)]
52. Gassner, G.; Patscheider, J.; Mayrhofer, P.H.; Sturm, S.; Scheu, C.; Mitterer, C. Tribological properties of nanocomposite CrC<sub>x</sub>/a-C:H thin films. *Tribol. Lett.* **2007**, *27*, 97–104. [[CrossRef](#)]
53. Yate, L.; Martinez-de-Olcoz, L.; Esteve, J.; Lousa, A. Effect of the bias voltage on the structure of nc-CrC/a-C:H coatings with high carbon content. *Surf. Coat. Technol.* **2012**, *206*, 2877–2883. [[CrossRef](#)]
54. Nygren, K.; Andersson, M.; Högström, J.; Frederiksson, W.; Edström, K.; Nyholm, L.; Jansson, U. Influence of deposition temperature and amorphous carbon on microstructure and oxidation resistance of magnetron sputtered nanocomposite Cr-C films. *Appl. Surf. Sci.* **2014**, *305*, 143–153. [[CrossRef](#)]
55. Nilsson, D.; Svahn, F.; Wiklund, U.; Hogmark, S. Low-friction carbon-rich carbide coatings deposited by co-sputtering. *Wear* **2003**, *254*, 1084–1091. [[CrossRef](#)]
56. Bobzin, K.; Lugscheider, E.; Maes, M. PVD-Niedertemperaturbeschichtung für Bauteile zur Integration tribologischer Funktionen in die Oberfläche. *Mat. Wiss. U. Werkstofftech.* **2004**, *35*, 843–850. [[CrossRef](#)]
57. Meng, Q.N.; Wen, M.; Mao, F.; Nedfors, N.; Jansson, U.; Zheng, W.T. Deposition and characterization of magnetron sputtered zirconium carbide films. *Surf. Coat. Technol.* **2013**, *232*, 876–883. [[CrossRef](#)]
58. Escudeiro, A.; Figueiredo, N.M.; Polcar, T.; Cavaleiro, A. Structural and mechanical properties of nanocrystalline Zr co-sputtered a-C(:H) amorphous films. *Appl. Surf. Sci.* **2015**, *325*, 64–72. [[CrossRef](#)]
59. Braic, M.; Braic, V.; Balaceanu, M.; Vladescu, A.; Zoita, C.N.; Titorencu, I.; Jinga, V.; Miculescu, F. Preparation and characterization of biocompatible Nb-C coatings. *Thin Solid Film.* **2011**, *519*, 4064–4068. [[CrossRef](#)]
60. Nedfors, N.; Tengstrand, O.; Lewin, E.; Furlan, A.; Eklund, P.; Hultman, L.; Jansson, U. Structural, mechanical and electrical-contact properties of nanocrystalline-NbC/amorphous-C coatings deposited by magnetron sputtering. *Surf. Coat. Technol.* **2011**, *206*, 354–359. [[CrossRef](#)]
61. Nedfors, N.; Tengstrand, O.; Flink, A.; Andersson, A.M.; Eklund, P.; Hultman, L.; Jansson, U. Reactive sputtering of NbC<sub>x</sub>-based nanocomposite coatings: An up-scaling study. *Surf. Coat. Technol.* **2014**, *253*, 100–108. [[CrossRef](#)]
62. Aouni, A.; Weisbecker, P.; Loi, T.H.; Bauer-Grosse, E. Search for new materials in sputtered V<sub>1-x</sub>C<sub>x</sub> films. *Thin Solid Film.* **2004**, *469*, 315–321. [[CrossRef](#)]
63. Krause, M.; Mücklich, A.; Wilde, C.; Vinnichenko, M.; Gemming, S.; Abrasonis, G. Structure, optical and mechanical properties of direct current magnetron sputtered carbon: Vanadium nanocomposite thin films. *Nanosci. Nanotechnol. Lett.* **2013**, *5*, 94–100. [[CrossRef](#)]
64. Heras, I.; Krause, M.; Abrasonis, G.; Pardo, A.; Endrino, J.L.; Guillén, E.; Escobar-Galindo, R. Advanced characterization and optical simulation for the design of solar selective coatings based on carbon:transition metal carbide nanocomposites. *Sol. Energy Mater. Sol. Cells* **2016**, *157*, 580–590. [[CrossRef](#)]
65. Stoyanov, P.; Schneider, J.; Rinke, M.; Ulrich, S.; Nold, E.; Dienwiebel, M.; Stüber, M. Microstructure, mechanical properties and friction behavior of magnetron-sputtered V-C coatings. *Surf. Coat. Technol.* **2017**, *321*, 366–377. [[CrossRef](#)]
66. Olofsson, J.; Gerth, J.; Nyberg, H.; Wiklund, U.; Jacobson, S. On the influence from micro topography of PVD coatings on friction behaviour, material transfer and tribofilm formation. *Wear* **2011**, *271*, 2046–2057. [[CrossRef](#)]
67. Hu, J.; Li, H.; Li, J.; Huang, J.; Kong, J.; Zhu, H.; Xiong, D. Structure, mechanical and tribological properties of TaC<sub>x</sub> composite films with different graphite powers. *J. Alloy. Compd.* **2020**, *832*, 153769. [[CrossRef](#)]
68. Luo, H.; Yazdi, M.A.P.; Chen, S.-C.; Sun, H.; Gao, F.; Heintz, O.; de Monteynard, A.; Sanchette, F.; Billard, A. Structure, mechanical and tribological properties, and oxidation resistance of TaC/a-C:H films deposited by high power impulse magnetron sputtering. *Ceram. Int.* **2020**, *46*, 24986–25000. [[CrossRef](#)]
69. Nilsson, D.; Stavlid, N.; Lindquist, M.; Hogmark, S.; Wiklund, U. The role of aluminum additions in the oxidation and wear of a TaC:C low-friction coating. *Surf. Coat. Technol.* **2009**, *203*, 2989–2994. [[CrossRef](#)]
70. Abad, M.D.; Sánchez-López, J.C.; Brizuela, M.; García-Luis, A.; Shtansky, D.V. Influence of carbon chemical bonding on the tribological behavior of sputtered nanocomposite TiBC/a-C coatings. *Thin Solid Film.* **2010**, *518*, 5546–5552. [[CrossRef](#)]
71. Lauridsen, J.; Nedfors, N.; Jansson, U.; Jensen, J.; Eklund, P.; Hultman, L. Ti-B-C nanocomposite coatings deposited by magnetron sputtering. *Appl. Surf. Sci.* **2012**, *258*, 9907–9912. [[CrossRef](#)]
72. Stueber, M.; Barna, P.B.; Simmonds, M.C.; Albers, U.; Leiste, H.; Ziebert, C.; Holleck, H.; Kovács, A.; Hovsepian, P.; Gee, I. Constitution and microstructure of magnetron sputtered nanocomposite coatings in the system Ti-Al-N-C. *Thin Solid Film.* **2005**, *493*, 104–112. [[CrossRef](#)]
73. Poltorak, C.; Stüber, M.; Leiste, H.; Bergmaier, A.; Ulrich, S. Study of (Ti,Zr)C:H/a-C:H nanocomposite thin film formation by low temperature reactive high power impulse magnetron sputtering. *Surf. Coat. Technol.* **2020**, *398*, 125958. [[CrossRef](#)]
74. Lewin, E.; Persson, P.O.A.; Lattemann, M.; Stüber, M.; Gorgoi, M.; Sandell, A.; Ziebert, C.; Schäfers, F.; Braun, W.; Halbritter, J.; et al. On the origin of a third spectral component of the C1s XPS-spectra for nc-TiC/a-C nanocomposite thin films. *Surf. Coat. Technol.* **2008**, *202*, 3563–3570. [[CrossRef](#)]
75. Magnuson, M.; Lewin, E.; Hultman, L.; Jansson, U. Electronic structure and chemical bonding of nanocrystalline-TiC/amorphous-C nanocomposites. *Phys. Rev. B* **2009**, *80*, 235108. [[CrossRef](#)]

76. El Mel, A.A.; Angleraud, B.; Gautron, E.; Granier, A.; Tessier, P.Y. XPS study of the surface composition modification of nc-TiC/C nanocomposite films under in situ argon ion bombardment. *Thin Solid Film.* **2011**, *519*, 3982–3985. [[CrossRef](#)]
77. Erdemir, A.; Donnet, C. Tribology of diamond-like carbon films: Recent progress and future prospects. *J. Phys. D Appl. Phys.* **2006**, *39*, R311–R327. [[CrossRef](#)]
78. Djoufack, M.H.; May, U.; Repphun, G.; Brögelmann, T.; Bobzin, K. Wear behaviour of hydrogenated DLC in a pin-on-disc model test under lubrication with different diesel fuel types. *Tribol. Int.* **2015**, *92*, 12–20. [[CrossRef](#)]
79. Donnet, C.; Erdemir, A. Tribology of Diamond-Like Carbon Films. Springer Science & Business Media: New York, NY, USA, 2008.
80. Mandal, P.; Ehiasarian, A.P.; Hovsepian, P.E. Lubricated sliding wear mechanism of chromium-doped graphite-like carbon coating. *Tribol. Int.* **2014**, *77*, 186–195. [[CrossRef](#)]
81. Mohrbacher, H.; Blanpain, B.; Celis, J.P.; Roos, J.R. Frictional behaviour of diamond-like carbon and diamond coatings in oscillating sliding. *Surf. Coat. Technol.* **1993**, *62*, 583–588. [[CrossRef](#)]
82. Ronkainen, H.; Varjus, S.; Holmberg, K. Tribological performance of different DLC coatings in water-lubricated conditions. *Wear* **2001**, *249*, 267–271. [[CrossRef](#)]
83. Tung, S.C.; Gao, H. Tribological characteristics and surface interaction between piston ring coatings and a blend of energy-conserving oils and ethanol fuels. *Wear* **2003**, *255*, 1276–1285. [[CrossRef](#)]
84. Podgornik, B.; Jacobson, S.; Hogmark, S. Influence of EP additive concentration on the tribological behaviour of DLC-coated steel surfaces. *Surf. Coat. Technol.* **2005**, *191*, 357–366. [[CrossRef](#)]
85. Kalin, M.; Vizintin, J. A comparison of the tribological behaviour of steel/steel, steel/DLC and DLC/DLC contacts when lubricated with mineral and biodegradable oils. *Wear* **2006**, *261*, 22–31. [[CrossRef](#)]
86. Haque, T.; Morina, A.; Neville, A.; Kapadia, R.; Arrowsmith, S. Non-ferrous coating/lubricant interactions in tribological contacts: Assessment of tribofilms. *Tribol. Int.* **2007**, *40*, 1603–1612. [[CrossRef](#)]
87. Grimm, W.; Wehnacht, V. Properties of super-hard carbon films deposited by pulsed arc process. *Vacuum* **2010**, *85*, 506–509. [[CrossRef](#)]
88. Kosarieh, S.; Morina, A.; Lainé, E.; Flemming, J.; Neville, A. Tribological performance and tribochemical processes in a DLC/steel system when lubricated in a fully formulated oil and base oil. *Surf. Coat. Technol.* **2013**, *217*, 1–12. [[CrossRef](#)]
89. Strmcnik, E.; Majdic, F.; Kalin, M. Water-lubricated behaviour of AISI 440C stainless steel and a DLC coating for an orbital hydraulic motor application. *Tribol. Int.* **2019**, *131*, 128–136. [[CrossRef](#)]
90. Barriga, J.; Kalin, M.; Van Acker, K.; Vercammen, K.; Ortega, A.; Leiaristi, L. Tribological performance of titanium doped and pure DLC coatings combined with a synthetic bio-lubricant. *Wear* **2006**, *261*, 9–14. [[CrossRef](#)]
91. Krzan, B.; Novotny-Farkas, F.; Vizintin, J. Tribological behavior of tungsten-doped DLC coating under oil lubrication. *Tribol. Int.* **2009**, *42*, 229–235. [[CrossRef](#)]
92. Yang, L.; Neville, A.; Brown, A.; Ransom, P.; Morina, A. Friction reduction mechanisms in boundary lubricated W-doped DLC coatings. *Tribol. Int.* **2014**, *70*, 26–33. [[CrossRef](#)]
93. Zhang, S.; Yue, W.; Kang, J.; Wang, Y.; Fu, Z.; Zhu, L.; She, D.; Wang, C. Ti content on the tribological properties of W/Ti-doped diamond-like carbon film lubricated with additives. *Wear* **2019**, *430–431*, 137–144. [[CrossRef](#)]
94. Bai, M.; Yang, L.; Li, J.; Luo, L.; Sun, S.; Inkson, B. Mechanical and tribological properties of Si and W doped diamond like carbon (DLC) under dry reciprocating sliding friction. *Wear* **2021**, *484*, 204046. [[CrossRef](#)]
95. Beake, B.D.; McMaster, S.J.; Liskiewicz, T.W.; Neville, A. Influence of Si- and W-doping on micro-scale reciprocating wear and impact performance of DLC coatings on hardened steels. *Tribol. Int.* **2021**, *160*, 107063. [[CrossRef](#)]
96. Scharf, T.W.; Singer, I.L. Role of the transfer film on the friction and wear of metal carbide reinforced amorphous carbon coatings during run-in. *Tribol. Lett.* **2009**, *36*, 43–53. [[CrossRef](#)]
97. Ciarsolo, I.; Fernández, X.; Ruiz de Gopegui, U.; Zubizarreta, C.; Abad, M.D.; Mariscal, A.; Caretti, I.; Jiménez, I.; Sánchez-López, J.C. Tribological comparison of different C-based coatings in lubricated and unlubricated conditions. *Surf. Coat. Technol.* **2014**, *257*, 278–285. [[CrossRef](#)]
98. Abad, M.D.; Sánchez-López, J.C.; Cusnir, N.; Sanjines, R. WC/a-C nanocomposite thin films: Optical and electrical properties. *J. Appl. Phys.* **2009**, *105*, 033510. [[CrossRef](#)]
99. Oláh, N.; Fogarassy, Z.; Furkó, M.; Balászi, C.; Balászi, K. Sputtered nanocrystalline ceramic TiC/amorphous C thin films as potential materials for medical applications. *Ceram. Int.* **2015**, *41*, 5863–5871. [[CrossRef](#)]
100. Park, Y.S.; Kim, N.-H. TiC/a-C nano composite films fabricated by using closed-field unbalanced magnetron sputtering for biomedical applications. *J. Korean Phys. Soc.* **2019**, *75*, 380–384. [[CrossRef](#)]
101. Xiao, Y.; Hwang, J.-Y.; Sun, Y.-K. Transition metal carbide-based materials: Synthesis and applications in electrochemical energy storage. *J. Mater. Chem. A* **2016**, *4*, 10379–10393. [[CrossRef](#)]
102. Qiu, F.; He, P.; Jiang, J.; Zhang, X.; Tong, S.; Zhou, H. Ordered mesoporous TiC-C composites as cathode materials for Li-O<sub>2</sub> batteries. *Chem. Commun.* **2016**, *52*, 2713. [[CrossRef](#)]
103. Wang, H.Q.; Zhou, Q.; Ou, Y.X.; Liao, B.; Zhang, X.; Hua, Q.S.; Ouyang, X.P.; Luo, C.W. Tribocorrosion behaviors of nc-TiC/a-C:H nanocomposite coatings: In-Situ electrochemical response. *Thin Solid Film.* **2021**, *730*, 138719. [[CrossRef](#)]
104. Oláh, N.; Fogarassy, Z.; Sulyok, A.; Szívós, J.; Csanádi, T.; Balászi, K. Ceramic TiC/a:C protective nanocomposite coatings: Structure and composition versus mechanical properties and tribology. *Ceram. Int.* **2016**, *42*, 12215–12220. [[CrossRef](#)]
105. Oláh, N.; Fogarassy, Z.; Sulyok, A.; Veres, M.; Kaptay, G.; Balászi, K. TiC crystallite formation and the role of interfacial energies on the composition during the deposition process of TiC/a:C thin films. *Surf. Coat. Technol.* **2016**, *302*, 410–419. [[CrossRef](#)]

106. Balászi, K.; Balászi, C. Application of sputtered ceramic TiC/a:C thin films with different structures by changing the deposition parameters. *Int. J. Appl. Ceram. Technol.* **2022**, *19*, 753–761. [[CrossRef](#)]
107. Bauer, C. *Superharte, Unterschiedlich Gradierte PVD-Kohlenstoffsichten Mit Und Ohne Zusatz Von Titan Und Silizium*, Wissenschaftliche Berichte FZKA 6740, Forschungszentrum Karlsruhe in der Helmholtz-Gemeinschaft; Forschungszentrum Karlsruhe GmbH: Karlsruhe, Germany, 2003.
108. Stueber, M.; Ziebert, C.; Leiste, H.; Ulrich, S.; Sanz, C.; Fuentes, E.; Etxarri, I.; Solay, M.; Garcia, A.; Barna, P.B.; et al. Wear Studies and Cutting Tests of Ti-Al-N-C Nanocomposite Coatings in Milling Operations—Technical Communication. *Mach. Sci. Technol.* **2009**, *13*, 122–141. [[CrossRef](#)]
109. Erdemir, A.; Martin, J.M. Superior wear resistance of diamond and DLC coatings. *Curr. Opin. Solid State Mater. Sci.* **2018**, *22*, 243–254. [[CrossRef](#)]
110. Buckley, D.H.; Miyoshi, K. Friction and wear of ceramics. *Wear* **1984**, *100*, 333–353. [[CrossRef](#)]
111. Jahanmir, S. *Friction and Wear of Ceramics*. CRC Press: Boca Raton, FL, USA, 1993.
112. Wallstabe, R. On the tribological behaviour of SiC and alumina mated against different steels under dry sliding conditions. *Tribol. Lett.* **2011**, *44*, 247–257. [[CrossRef](#)]
113. Muratov, V.A.; Fischer, T.E. Tribochemical polishing. *Ann. Rev. Mater. Sci.* **2000**, *30*, 27–51. [[CrossRef](#)]
114. Zhu, Z.; Muratov, V.; Fischer, T.E. Tribochemical polishing of silicon carbide in oxidant solution. *Wear* **1999**, *225*, 848–856. [[CrossRef](#)]
115. Jahnke, H.; Schoenborn, M. Electrochemical corrosion measurements in motor fuels based on methanol and ethanol. *Mater. Corros.* **1985**, *36*, 561–566. [[CrossRef](#)]
116. Alves Radi, P.; Vieira, A.; Manfroio, L.; Carvalho de Farias Nass, K.; Ramirez Ramos, M.A.; Leite, P.; Martins, G.V.; Jofre, J.B.F.; Vieira, L. Tribocorrosion and corrosion behavior of stainless steel coated with DLC films in ethanol with different concentrations of water. *Ceram. Int.* **2019**, *45*, 9686–9693. [[CrossRef](#)]
117. Dienwiebel, M.; Poehlmann, K.; Scherge, M. Origins of the wear resistance of AlSi cylinder bore surfaces studies by surface analytical tools. *Tribol. Int.* **2007**, *40*, 1597–1602. [[CrossRef](#)]
118. Costa, H.L.; Hutchings, I.M. Hydrodynamic lubrication of textured steel surfaces under reciprocating sliding conditions. *Tribol. Int.* **2007**, *40*, 1227–1238. [[CrossRef](#)]
119. Zhou, S.; Wang, L.; Xue, Q. Testing atmosphere effect on friction and wear behaviors of duplex TiC/a-C(Al) nanocomposite carbon-based coating. *Tribol. Lett.* **2012**, *47*, 435–446. [[CrossRef](#)]
120. Li, H.; Xu, T.; Wang, C.; Chen, J.; Zhou, H.; Liu, H. Tribochemical effects on the friction and wear behaviors of a-C:H and a-C films in different environment. *Tribol. Int.* **2007**, *40*, 132–138. [[CrossRef](#)]